



## Simulation of Biceps Femoris Muscle Growth Based on Stretch Using a Multiscale Model

S. Javadi<sup>1</sup>, A. Jaamialahmadi<sup>1\*</sup>, A. Daneshmehr<sup>2</sup>, M. Azadvari<sup>3</sup>, S. Nekoonam<sup>4</sup>

<sup>1</sup> Department of Mechanical Engineering, Faculty of Engineering, Ferdowsi University of Mashhad, Mashhad, Iran.

<sup>2</sup> School of Mechanical Engineering, University of Tehran, Tehran, Iran.

<sup>3</sup> Department of Physical Medicine and Rehabilitation, Tehran University of Medical Sciences, Tehran, Iran.

<sup>4</sup> Department of Anatomy, School of Medicine, Tehran University of Medical Sciences, Tehran, Iran.

### Review History:

Received: 17 Jan. 2019

Revised: 29 Jul. 2019

Accepted: 2 Sep. 2019

Available Online: 11 Nov. 2019

### Keywords:

Soft tissue growth

Finite element analysis

Hyperelastic

Musculoskeletal

Simulation

**ABSTRACT:** Understanding the process of muscle tissue growth is important to professionals who are involved in curing musculoskeletal disorders, physical medicine and rehabilitation specialists and orthopedic surgeons. This article investigates the development of a musculoskeletal cell and also determining the vulnerable areas of biceps femoris muscles due to passive strains applied on it. By decomposing the deformation gradient tensor to two parts, the elastic and growth, the finite growth relations have been applied for an isotropic hyperelastic muscle material behavior. Consequently, the continuum relations were combined with the growth evolution equation where a series of mechanobiological relations were obtained. To solve them, a FORTRAN user-defined material subroutine (UMAT) for the finite element Abaqus software was written and executed. The biceps femoris – long head muscle was simulated based on a 6-week period assuming as a cylinder with 10% increase in initial length. Results of the simulation indicate that maximum strains occur in the surfaces, not inside the muscle. They reach 1.045 near the proximal muscle-tendon junction in the posterior layer and 1.06 in distal muscle-junction in interior surface. Also, these results can help a correct and optimal treatment, patient's rehabilitation and orthopedic surgeries.

### 1- Introduction

One of the most common musculoskeletal problems is the shortening of hamstring muscles, which can be caused by various factors such as inactivity, chronic neurological diseases or spinal cord injury. This muscle shortening results in the patient's limited range of motion and numerous clinical problems [1]. To treat this disease, the muscle must be stretched in accordance with physiotherapy method to grow. The key question is how much and where are the maximal stretching locations during muscle growth? What is the process of muscle growth over time? The main unit of any muscle tissue is the sarcomere, which consists of two groups of actin and myosin. When the muscle is stretched, it results in a gap between these two groups. In this study, by applying soft tissue growth simulation, in addition to identifying the accurate location of the maximum stretch during growth process, the optimal time duration care of the muscle has been determined.

### 2- Methods

In order to simulate the growth of muscle, a single cubic element was considered as a skeletal muscle cell. Then the governing equations obtained by combining the continuum mechanics and growth evolution, were coded in an User-defined MATerial (UMAT) subroutine written in FORTRAN. The numerical simulation was performed in Abaqus/implicit

software in conjunction with a UMAT for soft tissue behaviour. Finally, a cylinder was considered as the Biceps femoris long head, which is one of the hamstring muscles, and its growth and severe strains were investigated. This simulation is based on a continuum model developed by Zöllner et al. [2]. Hence, the basic equations of this model are shown below.

One of the most important assumptions required for finite growth is decomposition of deformation gradient tensor, Such that

$$\mathbf{F} = \mathbf{F}_e \mathbf{F}_g, \quad \mathbf{F}_e = \mathbf{F} \mathbf{F}_g^{-1} \quad (1)$$

In this simulation, muscle growth is modeled only by increasing or decreasing the sarcomeres along the fibers, therefore, an inelastic deformation gradient proposed for this growth type is as follows [2]

$$\mathbf{F}_g = \mathbf{I} + [\mathcal{G} - 1] \mathbf{n}_0 \otimes \mathbf{n}_0 \quad (2)$$

where  $\mathbf{I}$  is the identity tensor,  $\mathbf{n}_0$  is the initial material direction, and  $\mathcal{G}$  is a growth variable that represents the relative serial sarcomere number. In order to extend simple equations for soft tissue, it is assumed that such growth to be homogeneous with isotropic properties. In addition, a strain energy function of Neo-Hookean type is adopted, as

\*Corresponding author's email: jaami-a@um.ac.ir.com



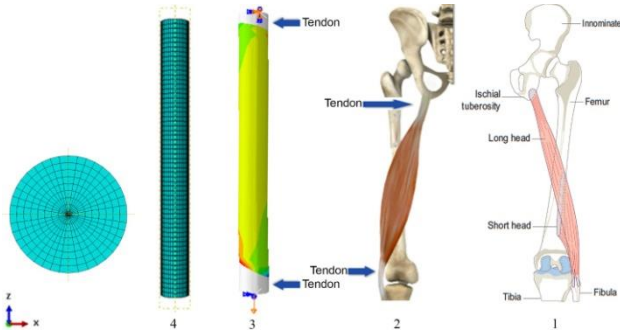


Fig. 1. Finite element model of the assumed cylindrical shape muscle

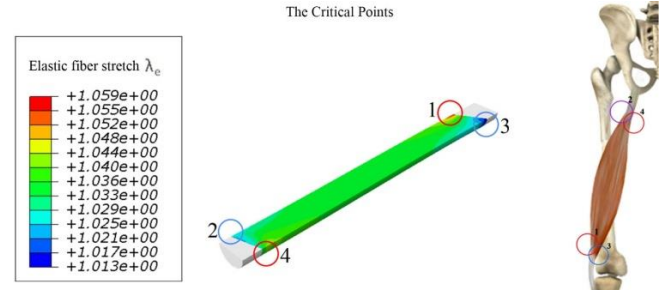


Fig. 3. The longitudinal-section view of the muscle after stretching

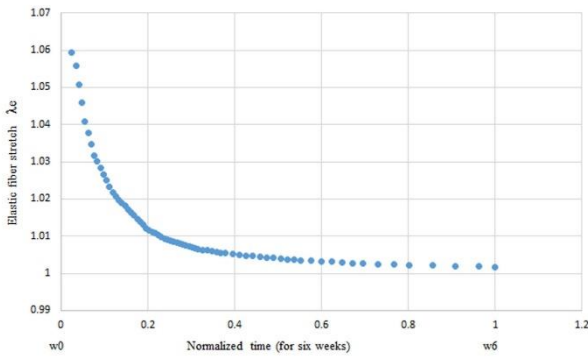


Fig. 2. Dynamic changes in the sarcomere length.

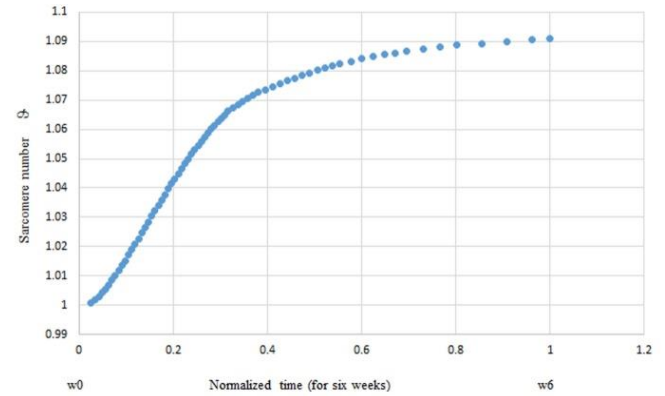


Fig. 4. Dynamic changes in the sarcomere number

$$\psi = \frac{1}{2}c_1 \ln^2(J_e) + \frac{1}{2}c_2 [\mathbf{C}_e : \mathbf{I} - 3 - 2\ln(J_e)] \quad (3)$$

where  $c_1$  and  $c_2$  are the Lamé constants,  $\mathbf{C}_e$  is the elastic right Cauchy green tensor, and  $J_e$  denotes elastic volume change. The second Piola-Kirchhoff stress tensor  $\mathbf{S} = 2\partial\psi/\partial\mathbf{C}$  and the fourth-order Lagrangian elastic tensor  $\mathbf{L} = 4\partial^2\psi/\partial\mathbf{C} \otimes \partial\mathbf{C}$  are derived from the second law of thermodynamics. Furthermore, the Kirchhoff stress  $\boldsymbol{\tau} = \mathbf{F}\mathbf{S}\mathbf{F}^t$  is obtained using a push-forward operation. In this simulation, the evolution Eq. (4) is adopted to calculate the relative serial sarcomere number [2].

$$\dot{\mathcal{G}} = k_g(\mathcal{G}) \phi_g(\lambda_e) \quad (4)$$

where  $k_g = 1/\tau [\mathcal{G}^{\max} - \mathcal{G}/\mathcal{G}^{\max} - 1]^\gamma$  is the adaptation function and  $\phi_g = \langle \lambda_e - \lambda_{\text{crit}} \rangle$  is the adaptation criterion. To solve the nonlinear equations, a finite element computational model was implemented in conjunction with an user subroutine by implicit solver of the Abaqus/standard version 6.13. The relative sarcomere number  $\mathcal{G}$  is introduced as an internal vari-

able and then its evolution Eq. (4) is solved using a finite-difference approximation method. After determining the amount of new sarcomere  $\mathcal{G}$ , the growth gradient deformation  $\mathbf{F}_g$  is calculated from Eq. (2) and the elastic gradient deformation  $\mathbf{F}_e$  from Eq. (1), too. Finally, the true Cauchy stress  $\boldsymbol{\sigma}^{\text{abaqus}} = \boldsymbol{\tau}/J$ , which the user-defined subroutine in Abaqus/standard utilizes, is calculated to be applied to the muscle

### 3- Cylindrical shape muscle model

A cylindrical shape muscle finite element model with a height of 400 mm and a diameter of 20 mm is illustrated in Fig. 1. After a mesh sensitivity procedure, a model with 53487 elements including 38556 linear hexagonal elements of type C3D8 and 14931 linear wedge elements of type C3D6, was generated. For increasing computational efficiency in modeling, because a tendon is much stiffer than muscle tissue, it has been assumed as a rigid member [3]. Biceps femoris's fibers are drawn from distal to proximal in a closed and parallel manner [4]. In this study, this direction is aligned with the stretch axis. The head of the muscle which is attached to the Fibula bone are considered as a movable and the head of the muscle is attached to the ischial tuberosity bone as a fixed boundary condition as well. The boundary conditions and the material parameter are shown in Fig. 1 and Table 1 respectively.

**Table 1. The material parameters**

$c_1$	$c_2$	$\tau$	$\gamma$	$\mathcal{G}^{\max}$	$\lambda_{crit}$
16 kPa	4 kPa	0.5	2.0	1.1	1.01

#### 4- Results and Discussion

The simulation results of the dynamic changes in sarcomere length for the element with maximum amounts of elastic stretch are plotted in Fig. 2. The graph was drawn in response to a 10% increase in muscle length for a 6-week treatment period. According to this graph, the elastic stretch  $\lambda_e$  decreases from 1.06 to 1 after this time duration. Furthermore, a significant decrease in the elastic fiber stretch during the first two weeks not only does ease the pain but also indicates a high chance of injury at this time.

Fig. 3 shows the cross-sectional view of the muscle after stretching. The red circles represent the maximum stretch location and the blue circles indicate the minimum ones. As can be seen from this figure, these points are the closest points to the myotendinous junction and are located on the inner and outer surfaces of the muscle. De Smet and Best [5] applied magnetic resonance imaging to 15 athletes with hamstring muscle injuries. They showed that all of these injuries occurred adjacent to myotendinous junction.

Fig. 4 shows the dynamic changes in the number of sarcomeres that were normalized versus to 6 weeks of treatment in response to a 10% increase in muscle length. The growth of sarcomeres was high in the early weeks, leading to a greater flexibility rate than the last weeks.

#### 5- Conclusion

In this study, a biceps femoris long head muscle considered as a cylinder with a model of soft tissue growth was simulated numerically. In this study, a numerical model of soft tissue

growth was simulated on a cylinder assumed as a biceps femoris long head muscle. An isotropic behavior and a Neo-Hookean elastic model were used for the muscle material. The results showed that the rapid growth of sarcomeres, which lead to severe pain, occurs within the first weeks of treatment duration. Furthermore, the most critical points that tolerate maximum stretch are located in the proximal area on the posterior surface and the distal area on the interior surface of the muscle and on the myotendinous junction. The results of this simulation are in accordance with the results of an investigating of clinical magnetic resonance imaging for 15 athletes with hamstring muscle injuries.

#### References

- [1] W.E. Prentice, *Rehabilitation Techniques for Sports Medicine and Athletic Training with Laboratory Manual and ESims Password Card*, McGraw-Hill Education, 2005.
- [2] A.M. Zöllner, O.J. Abilez, M. Böl, E. Kuhl, Stretching skeletal muscle: chronic muscle lengthening through sarcomerogenesis, *PloS one*, 7(10) (2012) e45661.
- [3] A.M. Zöllner, J.M. Pok, E.J. McWalter, G.E. Gold, E. Kuhl, On high heels and short muscles: a multiscale model for sarcomere loss in the gastrocnemius muscle, *Journal of theoretical biology*, 365 (2015) 301-310.
- [4] N. Palastanga, R. Soames, *Anatomy and human movement, structure, and function with pageburst access*, 6: anatomy and human movement, Elsevier Health Sciences, 2011.
- [5] A.A. De Smet, T.M. Best, MR imaging of the distribution and location of acute hamstring injuries in athletes, *American Journal of Roentgenology*, 174(2) (2000) 393-399.

